[6] a) R. G. Chapman, J. C. Sherman, *J. Am. Chem. Soc.* **1995**, *117*, 9081–9082; b) R. G. Chapman, G. Olovsson, J. Trotter, J. C. Sherman, *J. Am. Chem. Soc.* **1998**, *120*, 6252–6260.

[7] The value -0.9 is δ(pyrazine in **3**·pyrazine·MeOAc) – δ(pyrazine in **3**·2pyrazine). The value $+0.19$ is $\delta(\mathrm{CH_3COC}H_3$ in **3**·pyrazine·MeOAc) – $\delta(\mathrm{CH_3COC}H_3$ in **3**·2MeOAc). The value $+0.16$ is $\delta(\mathrm{C}H_3\mathrm{COCH_3}$ in **3**·pyrazine·MeOAc) – $\delta(\mathrm{C}H_3\mathrm{COCH_3}$ in **3**·2MeOAc).

[8] For encapsulation of two or more guest molecules in a single large chamber, see a) F. C. Tucci, D. M. Rudkevich, J. Rebek, Jr., *J. Am. Chem. Soc.* **1999**, *121*, 4928–4929; b) R. Meissner, X. Garcias, S. Mecozzi, J. Rebek, Jr., *J. Am. Chem. Soc.* **1997**, *119*, 77–85; c) T. Heinz, D. Rudkevich, J. Rebek, Jr., *Nature* **1998**, *394*, 764–766; d) J. Kang, J. Rebek, Jr., *Nature* **1997**, *385*, 50–52; e) J. Kang, J. Santamaria, G. Hilmersson, J. Rebek, Jr., *J. Am. Chem. Soc.* **1998**, *120*, 7389–7390; f) N. Chopra, J. C. Sherman, *Angew. Chem.* **1999**, *111*, 2109–2111; *Angew. Chem. Int. Ed.* **1999**, *38*, 1955–1957.

[9] a) R. G. Chapman, N. Chopra, E. D. Cochien, J. C. Sherman, *J. Am. Chem. Soc.* **1994**, *116*, 369–370; b) R. G. Chapman, J. C. Sherman, *J. Org. Chem.* **1998**, *63*, 4103–4110.

[10] The ^{1}H NMR spectra of **1** and DBU in $\mathrm{CHCl_3/CDCl_3}$ (1/1) at 298 K gave signals for encapsulated $\mathrm{CHCl_3}$ ($\delta = 5.04$); thus the free species is **3**·2CHCl$_3$. Upon addition of MeOAc, a new signal for encapsulated $\mathrm{CHCl_3}$ ($\delta = 5.36$) appears, in addition to the new signals of encapsulated MeOAc and host; integration yields **3**·MeOAc·CHCl$_3$. Cooperativity appears at first to be lost in $\mathrm{CDCl_3}$, but this is because the second capsule is actually filled with $\mathrm{CDCl_3}$, which is "invisible" in the ^{1}H NMR spectra. See the Supporting Information for plots of [**3**·2CDCl$_3$], [**3**·MeOAc·CDCl$_3$], and [**3**·2MeOAc] as a function of $[\mathrm{MeOAc}]_{\mathrm{initial}}$.

[11] The formation of all complexes reported here is reversible; equilibrium is reached in minutes in [D$_5$]nitrobenzene at 373 K and in 24 h in $\mathrm{CDCl_3}$ at 298 K. For calculations of K_{rel}, $[\mathbf{1}]_{\mathrm{initial}} = 1.61\,\mathrm{mM}$; $[\mathrm{MeOAc}]_{\mathrm{initial}} = 32.2\,\mathrm{mM}$; $[\mathrm{CDCl_3}] = 12.5\,\mathrm{M}$; [**3**·CDCl$_3$·MeOAc] = 0.525 mM; [**3**·2MeOAc] = 0.972 mM; [**3**·2CDCl$_3$] = 0.113 mM; $[\mathrm{MeOAc}]_{\mathrm{free}} = 29.7\,\mathrm{mM}$. K_{rel} = [cap·MeOAc][CDCl$_3$]/[cap·CDCl$_3$][MeOAc], where cap = any capsule; for example, [cap·MeOAc] = [**3**·CDCl$_3$·MeOAc] + 2[**3**·2MeOAc]. See the Supporting Information for the derivation of this equation.

[12] R. G. Chapman, J. C. Sherman, *J. Am. Chem. Soc.* **1998**, *120*, 9818–9826.

[13] R. G. Chapman, J. C. Sherman, *J. Am. Chem. Soc.* **1999**, *121*, 1962–1963.

A Two-Step Spin Crossover in [(TPA)Fe$^{\mathrm{III}}$(cat)]BPh$_4$**

A. Jalila Simaan, Marie-Laure Boillot,* Eric Rivière, Alain Boussac, and Jean-Jacques Girerd*

In our studies of mimics for intradiol catechol dioxygenase[1] we synthesized [(TPA)Fe(cat)]BPh$_4$ (**1**, TPA = tris(2-pyridylmethyl)amine, cat = catecholate dianion), a close analogue of [(TPA)Fe(DBC)]BPh$_4$ (**2**, DBC = 3,5-di-*tert*-butylcatecholate dianion) prepared first by Que et al.[2] The latter, in the presence of O$_2$, gives a nice example of intradiol dioxygenase activity with cleavage of the intradiol C–C bond.[2a] As a routine check of the spin state, we measured the magnetic susceptibility of **1** as a function of temperature and discovered that it exhibits a spin crossover,[3] and moreover one in two steps. We report here the preliminary study of this unusual phenomenon.

Elemental analysis confirmed that complex **1** is consistent with the formula [(TPA)Fe(cat)]BPh$_4$ and is unsolvated. The UV/Vis spectrum of **1** in acetonitrile/DMF (9/1) contains two broad ligand–metal charge transfer (LCMT) bands with maxima at 502 nm (2680 $\mathrm{M^{-1}\,cm^{-1}}$) and 808 nm (3890 $\mathrm{M^{-1}\,cm^{-1}}$), similar to those observed in other iron(III)-catecholato complexes.[2b] It may be inferred from this result that the cat ligand chelates the iron(III) ion in an analogous manner to DBC in **2**.[2a] The structure we propose for **1** is represented in Figure 1.

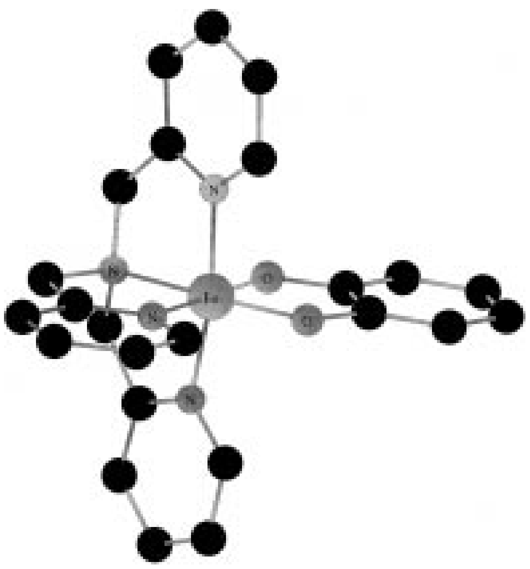

Figure 1. Proposed structure for the [(TPA)Fe(cat)]$^+$ ion.

The temperature dependence of $\chi_{\mathrm{M}}T$ (χ_{M} = molar magnetic susceptibility) of a microcrystalline sample of **1** (Figure 2) provides evidence for a spin crossover between $S = \frac{1}{2}$ (low spin) and $S = \frac{5}{2}$ (high spin) states of the iron(III) ion.[4, 5] The expected value of $\chi_{\mathrm{M}}T$ for the high-spin iron(III) ion is 4.375 $\mathrm{cm^3\,mol^{-1}\,K}$. As the room temperature value of $\chi_{\mathrm{M}}T$ is 4.14 $\mathrm{cm^3\,mol^{-1}\,K}$, it is expected that most of the iron(III) ions are in the $S = \frac{5}{2}$ state. From the data it can be estimated that about 3% of the molecules are in the low-spin state at room temperature. The value of $\chi_{\mathrm{M}}T$ is 0.49 $\mathrm{cm^3\,mol^{-1}\,K}$ at 45 K and stays nearly independent of temperature down to 5 K. This value is characteristic of low-spin iron(III) ions and hence of a complete spin conversion at low temperature. These data recorded at decreasing and increasing temperatures did not show any hysteresis effect. Between 45 and 175 K, the $\chi_{\mathrm{M}}T$ versus T curve reveals that the spin-crossover phenomenon takes place in two distinct steps centered at 79 and 106 K (Figure 2, inset). A rather abrupt transformation is observed between 45 and 94 K (80% of the conversion occur within

---

[*] Dr. M.-L. Boillot, Prof. J.-J. Girerd, A. J. Simaan, Dr. E. Rivière
Laboratoire de Chimie Inorganique, UMR CNRS 8613
Université Paris-Sud, 91405 Orsay (France)
Fax: (+33) 1-69-15-47-54
E-mail: mboillot@icmo.u-psud.fr, jjgirerd@icmo.u-psud.fr

Dr. A. Boussac
Section de Bioénergétique, URA CNRS 2096
CEA Saclay, 91191 Gif-sur-Yvette (France)

[**] Financial supports from the research fund TMR of the European Union (Contracts ERB-FMRX-CT 98-0199) and from the CNRS are gratefully acknowledged.

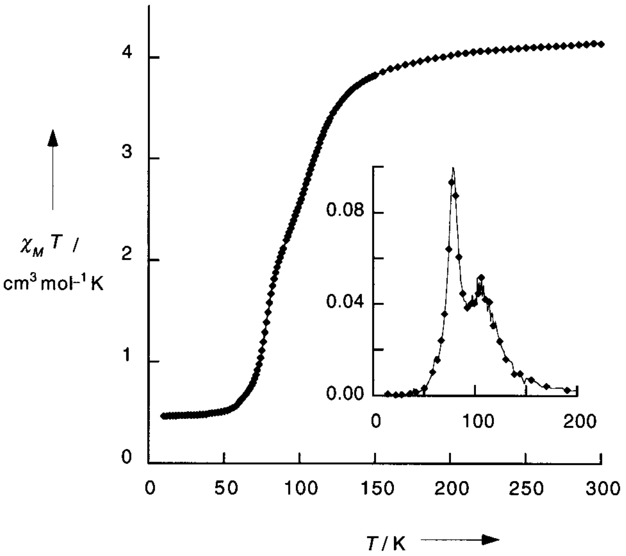

Figure 2. Variation of $\chi_M T$ with temperature for **1**. Inset: The first derivative of the $\chi_M T$ versus T curve.

an approximate 27 K range). Around 94 K ($\chi_M T$ = 2.32 cm^{3}mol^{-1}K), the transition curve presents an intermediate inflexion point corresponding to a high-spin fraction of about 48%. The spin crossover at higher temperatures is smoother. The fact that this magnetic behavior was found with different solid samples originating from different preparations allows us to discard the hypothesis of a 1:1 mixture of two crystalline phases exhibiting spin-crossover processes at different temperatures.

Two-step spin-crossover processes have been reported only in a few scarce iron(II) and iron(III) complexes.[6, 7] One possible origin of this peculiar behavior is the existence of two nonequivalent sites in the unit cell. For some of these compounds[6b, c, 7] the crystallographic structures at different temperatures substantiated this explanation. The complexes in the two local environments give rise to different spin-crossover processes. To address the origin of the magnetic behavior reported here, efforts are now directed to obtain crystals of **1** suitable for structural determination by X-ray diffraction.

The EPR spectra of **1** in the solid state have been recorded as a function of temperature (Figure 3). At 2.2 K the spectrum ($g_{\parallel}$ = 1.91, $g_{\perp}$ = 2.18) is characteristic of a low-spin axial iron(III) species.[4b, 8] This result demonstrates that the low-spin phase corresponds to a low-spin iron(III) catecholate complex. A possible low-spin iron(II) semiquinonate complex is ruled out because no radical-type signal was observed. At higher temperatures, a signal appears at low field while the low-spin signal disappears. It can be inferred from the magnetic data that this low-field signal, broadened by spin–spin interactions, is due to the high-spin fraction. The breadth of the signal forbids the evaluation of the zero-field splitting parameters. At low field and low temperatures, weak resonances are detected that we assigned to high-spin ferric impurities. Under the EPR experimental conditions the signals from these impurities are amplified, which means that they are present in a small amount only and hence could not be detected with magnetic measurements.

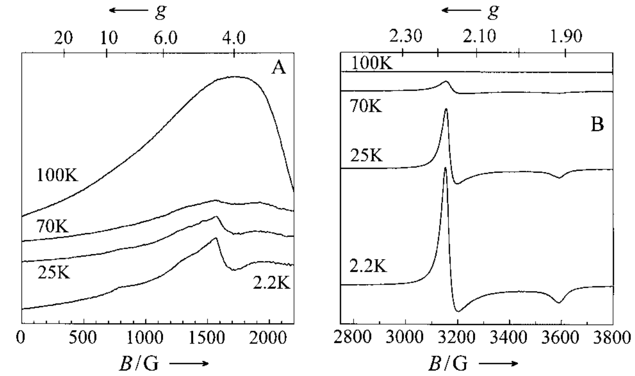

Figure 3. X-band EPR spectra of a powder sample of **1** as a function of temperature (2.2–100 K). A) Low-field region: gain = 10^4, frequency modulation = 100 kHz, amplitude modulation = 9.466 G, microwave power = 2×10^1 mW; B) high-field region: gain = 10^3, frequency modulation = 100 kHz, amplitude modulation 4.744 G, microwave power = 5.02×10^{-3} mW.

The magnetic susceptibility of **2**, recorded as a function of the temperature, shows a very smooth spin-crossover process.[9] This result could be due to the bulkiness of the *tert*-butyl groups which would reduce the cooperativity by keeping molecules separated.

We are now studying this two-step spin-crossover process of **1** by other spectroscopic methods. In particular, we are interested in the analysis of the intense LMCT bands throughout the temperature range of the spin crossover. Chemical variations of this iron(III) catecholate complex will be explored in order to modulate features of the associated spin-crossover process.

Experimental Section

TPA was prepared following the described procedure[10] but extracted with toluene and recrystallized from *n*-hexane rather than precipitated with $HClO_4$.

The synthesis of **1** was performed under an argon atmosphere. Catechol (56 mg, 0.50 mmol) was dissolved in CH_3OH (5 mL) and deprotonated by Et_3N (139 μL, 1 mmol); the solution was added to a mixture of $FeCl_3$ (80 mg, 0.49 mmol) and TPA (150 mg, 0.51 mmol) in methanol (15 mL). A dark blue, microcrystalline powder was precipitated by adding $NaBPh_4$ (170 mg, 0.49 mmol) in methanol and collected by filtration (yield 55%). Elemental analysis: $C_{42}H_{37}BFeN_4O_2$ (%): calcd: C 74.49, H 5.47, B 1.42, Fe 7.23, N 7.24; found: C 74.19, H 5.20, B 1.40, Fe 7.15, N 7.39.

Magnetic susceptibility measurements were carried out with a Quantum Design SQUID magnetometer (Model MPMS5S) calibrated against a palladium standard. The independence of the susceptibility value with regard to the applied magnetic field was checked at room temperature. EPR spectra were recorded at several temperatures with a Bruker ESP300 X-band spectrometer equipped with a Bruker ESR910 cryostat.

Received: July 21, 1999 [Z13762]

---

[1] a) P. Mialane, E. Anxolabéhère-Mallart, G. Blondin, A. Nivorojkine, J. Guilhem, L. Tchertanova, M. Cesario, N. Ravi, E. Bominaar, J. J. Girerd, E. Münck, *Inorg. Chim. Acta* **1997**, *263*, 367; b) P. Mialane, L. Tchertanova, F. Banse, J. Sainton, J. J. Girerd, *Inorg. Chem.*, in press; c) P. Mialane, PhD thesis, University of Paris-XI-Orsay (France), **1997**.

[2] a) H. G. Jang, D. D. Cox, L. Que, Jr, *J. Am. Chem. Soc.* **1991**, *113*, 9200; b) D. D. Cox, S. J. Benkovic, L. M. Bloom, F. C. Bradley, M. J. Nelson, L. Que, Jr, D. E. Wallick, *J. Am. Chem. Soc.* **1988**, *110*, 2026.

[3] P. Gütlich, A. Hauser, H. Spiering, *Angew. Chem.* **1994**, *106*, 2109; *Angew. Chem. Int. Ed. Engl.* **1994**, *33*, 2024.
[4] a) M. F. Tweedle, L. J. Wilson, *J. Am. Chem. Soc.* **1976**, *98*, 16, 4824; b) M. D. Timken, D. N. Hendrickson, E. Sinn, *Inorg. Chem.* **1985**, *24*, 3947.
[5] W. O. Koch, V. Schünemann, M. Gerdan, A. X. Trautwein, H. J. Krüger, *Chem. Eur. J.* **1998**, *4*, 686.
[6] a) C. P. Köhler, R. Jakobi, E. Meissner, L. Wiehl, H. Spiering, P. Gütlich, *J. Phys. Chem. Solids* **1990**, *51*, 239; b) D. Boinnard, A. Bousseksou, A. Dworking, J. M. Savariault, F. Varret, J. P. Tuchagues, *Inorg. Chem.* **1994**, *33*, 271; c) Y. Garcia, PhD thesis, University of Bordeaux I (France), **1999**; d) J. A. Real, H. Bolvin, A. Bousseksou, A. Dworkin, O. Kahn, F. Varret, J. Zarembowitch, *J. Am. Chem. Soc.* **1992**, *114*, 4650.
[7] V. V. Zelentsov, *Sov. Sci. Rev. Sect. B.* **1987**, *10*, 485.
[8] C. Kim, K. Chen, J. Kim, L. Que, Jr, *J. Am. Chem. Soc.* **1997**, *119*, 5964.
[9] A. J. Simaan, unpublished results.
[10] B. G. Gafford, R. A. Holwerda, *Inorg. Chem.* **1989**, *28*, 60.

O–H···Pt^{II}: Hydrogen Bond with a Strong Dispersion Component[**]

Jiří Kozelka,[*] Jacqueline Bergès, Roger Attias, and Jann Fraitag

In the past decade, crystallographic and spectroscopic evidence has accumulated showing that d^8 metal ions such as platinum(II) are capable of acting as hydrogen-bond acceptors.[1, 2] One may ask whether water could undergo similar hydrogen bond like interactions with solvated platinum complexes. We report here an ab initio study, at the Møller-Plesset second-order perturbation (MP2) level, of the interaction between a water molecule and two platinum(II) complexes $[Pt(NH_3)_4]^{2+}$ (**1**) and *trans*-$[Pt(OH)_2(NH_3)_2]$ (**2**). Our calculations indicate that a linear HO–H···Pt interaction is stabilized by a strong dispersion component. In the case of the HO–H···$Pt(NH_3)_4{}^{2+}$ interaction, the dispersion component considerably reduces the electrostatic repulsion, while for the HO–H···$Pt(OH)_2(NH_3)_2$ approach, it adds to the electrostatic attraction, giving rise to a hydrogen bond like interaction with a dissociation energy of about 4 kcal mol^{-1}. It is suggested for the previously reported complex *cis*-$[PtBr_2(gly\text{-}N)_2]\cdot H_2O$ (gly = NH_2CH_2COOH) that a similar hydrogen bond between a water molecule and an uncharged platinum central atom occurs in the solid state. Therefore, not only in anionic but also in electrically neutral platinum(II) complexes can the platinum atom act as a hydrogen-bond acceptor.

Two approaches of a water molecule to **1** or **2** along the *z* axis (defined as the normal to the platinum coordination plane through the Pt atom) were considered: approach I with the O atom oriented toward Pt and approach II with the O–H vector directed toward Pt, as shown for complex **2** in Figure 1.

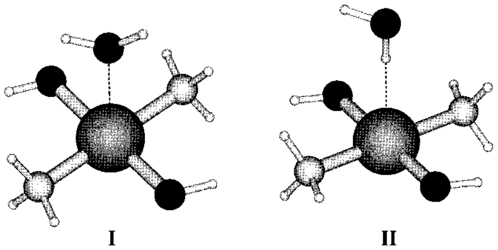

Figure 1. Approaches of H_2O, using complex **2** as an example. Approach I: O atom directed toward Pt; approach II with O–H vector directed toward Pt.

The interaction energies at the Hartree–Fock (E_{HF}) and at the MP2 (E_{MP2}) levels were evaluated as the difference between the total energy of the two interacting species and the sum of the total energies of the individual molecules, corrected for the basis set superposition error. In addition, an estimate of the electrostatic component (E_{ES}) was obtained as the sum of Coulomb terms q_iq_j/r_{ij} between atomic charges determined by optimizing the fit to the MP2 electrostatic potential of the isolated molecules. To an approximation, the interaction energy E_{MP2} can be considered to be the sum of the electrostatic (E_{ES}), exchange-repulsion (E_{EX}), polarization (E_{POL}), and charge-transfer (E_{CT}) components, plus the contribution of electron correlation effects E_{CORR}[4–6] (Eq. 1).

$$E_{MP2} = E_{ES}+E_{EX}+E_{POL}+E_{CT}+E_{CORR} \quad (1)$$

It is common practice to associate the interaction energy determined at the Hartree–Fock level E_{HF} with the sum $E_{ES}+E_{EX}+E_{POL}+E_{CT}$.[5] The difference $E_{MP2} - E_{HF}$ can be therefore used as an estimate for E_{CORR}. In Figure 2, the interaction energies E_{MP2}, E_{HF}, and E_{ES} are plotted against the Pt···O separation, together with the differences $E_{MP2} - E_{HF}$ and $E_{HF} - E_{ES}$.

Approach I (Figure 2a, b): In approach I, both E_{HF} and E_{MP2} curves quite closely follow the E_{ES} curve at long and intermediate distances, indicating that the interaction is mainly determined by electrostatic (long-range) and exchange-repulsion (short-range) energy. For the approach I/**1** the electrostatic energy is negative, giving rise to a profound (−11 kcal mol^{-1}) energy minimum at a Pt···O distance of about 3.3 Å, whereas approach I/**2** is purely repulsive. Agreement with the deep minimum for approach I/**1** is found in the Cambridge Crystallographic Data Centre (CCDC), which contains several entries of dicationic platinum(II) tetraamine complexes with axial water ligands at distances between 3 and 3.5 Å. The structure of $[Pt(py)_4]Cl_2\cdot 3H_2O$ (py = pyridine), determined by neutron diffraction,[7] (Figure 3) for example, features a square-planar PtN_4 coordination, which is extended

---

[*] Dr. J. Kozelka, Dr. R. Attias, J. Fraitag
Laboratoire de Chimie et Biochimie Pharmacologiques
et Toxicologiques, UMR CNRS 8601
45, rue des Saints-Pères, 75270 Paris (France)
Fax: (+33) 1-42-86-83-87
E-mail: kozelka@biomedicale.univ-paris5.fr
Dr. J. Bergès
Laboratoire de Chimie Théorique
Université Pierre et Marie Curie
4, place Jussieu, 75005 Paris (France)

[**] We are indebted to Drs. J. Langlet, P. Pyykkö, A. Pullman, J. Caillet, and C. Giessner-Prettre for stimulating discussions and helpful comments. Computer time from the IDRIS center of CNRS is gratefully acknowledged.

0570-0833/00/3901-0198 $ 17.50+.50/0